4150 *Biochemistry* **2009,** *48,* 4150–4158
DOI:10.1021/bi900168m

BIOCHEMISTRY
including biophysical chemistry & molecular biology
Article

Steroid and Protein Ligand Binding to Cytochrome P450 46A1 as Assessed by Hydrogen−Deuterium Exchange and Mass Spectrometry†

Wei-Li Liao,[‡,§] Nathan G. Dodder,[§] Natalia Mast,[∥] Irina A. Pikuleva,[∥] and Illarion V. Turko*[,‡,§]

[‡]*Center for Advanced Research in Biotechnology, University of Maryland Biotechnology Institute, Rockville, Maryland 20850,* [§]*National Institute of Standards and Technology, Gaithersburg, Maryland 20899, and* [∥]*Department of Ophthalmology and Visual Sciences, Case Western Reserve University, Cleveland, Ohio 44106*

Received February 2, 2009. Revised Manuscript Received March 24, 2009

ABSTRACT: Cytochrome P450 46A1 (CYP46A1) is a key enzyme responsible for cholesterol elimination from the brain. This P450 can interact with different steroid substrates and protein redox partners. We utilized hydrogen−deuterium (H-D) exchange mass spectrometry for investigating CYP46A1-ligand interactions. First, we tested the applicability of the H-D exchange methodology and assessed the amide proton exchange in substrate-free and cholesterol-sulfate-bound P450. The results showed good correspondence to the available crystal structures and prompted investigation of the CYP46A1 interactions with the two steroid substrates cholesterol and 24*S*-hydroxycholesterol and the protein redox partner adrenodoxin (Adx). Compared to substrate-free P450, four peptides in cholesterol-bound CYP46A1 (65−80, 109−116, 151−164, and 351−361) and eight peptides in 24*S*-hydroxycholesterol-bound enzyme (50−64, 65−80, 109−116, 117−125, 129−143, 151−164, 260−270, and 364−373) showed altered deuterium incorporation. Most of these peptides constitute the enzyme active site, whereas the 351−361 peptide is from the region putatively interacting with the redox partner Adx. This also defines the proximal (presumably water) channel that opens in CYP46A1 upon substrate binding. Reciprocal studies of Adx binding to substrate-free and cholesterol-sulfate-bound CYP46A1 revealed changes in the deuteration of the Adx-binding site 144−150 and 351−361 peptides, active site 225−239 and 301−313 peptides, and in the 265−276 peptide, whose functional role is not yet known. The data obtained provide structural insights into how substrate and redox partner binding are coordinated and linked to the hydration of the enzyme active site.

The initial reactions in cholesterol biotransformation to bile acids and steroid hormones are catalyzed by a group of hemoproteins called cytochrome P450s (P450s or CYPs[1]) (*1*,*2*). The focus of the present work is on CYP46A1, which catalyzes the first step in the major pathway of cholesterol elimination from the brain. CYP46A1 converts cholesterol to 24*S*-hydroxycholesterol. Unlike cholesterol, 24*S*-hydroxycholesterol can cross the blood−brain barrier and be transported to the liver for further degradation to bile acids (*3*,*4*). The significance of CYP46A1 may not be limited to its involvement in cholesterol degradation. 24*S*-Hydroxycholesterol is a potent activator of the LXR receptors in cultured cells and mice (*5*); therefore, CYP46A1 may play a regulatory role by producing a biologically active product. It is also possible that CYP46A1 may be involved in subsequent metabolism of 24*S*-hydroxycholesterol. *In vitro*, CYP46A1 was found to further oxidize 24*S*-hydroxycholesterol to 24,25- and 24,27-dihydroxycholesterols with the catalytic efficiency ∼10-fold higher than that of cholesterol hydroxylation (*6*,*7*). CYP46A1 activity *in vitro* can be reconstituted with either NADPH-cytochrome P450 oxidoreductase (CPR), the redox partner for microsomal P450s (*6*), or with adrenodoxin reductase (AdR) and adrenodoxin (Adx) constituting the mitochondrial electron transfer chain (Pikuleva I. A., personal communication). Thus, it is possible that *in vivo* CYP46A1 interacts with different steroids and redox partners. Crystal structures of the substrate-free and cholesterol-sulfate-bound CYP46A1 have been recently determined and revealed that the enzyme undergoes significant conformational changes upon substrate binding (*7*). This conformational flexibility prompted the current study accessing the molecular

†This work was supported in part by grants from the National Institutes of Health GM062882 and AG024336 (to I.A.P.) and by the Jules and Doris Stein Professorship from Research to Prevent Blindness Foundation (to I.A.P.).

*To whom correspondence should be addressed. Tel: 240-314-6257. Fax: 240-314-6225. E-mail: turko@umbi.umd.edu.

[1]Abbreviations: CYP, cytochrome P450; CYP46A1, cytochrome P450 46A1; CPR, NADPH-cytochrome P450 oxidoreductase; AdR, adrenodoxin reductase; Adx, adrenodoxin; H-D, hydrogen−deuterium; ESI, electrospray ionization; MALDI, matrix assisted laser desorption ionization; MS, mass spectrometry; TOF, time-of-flight; TFA, trifluoroacetic acid.

 Published on Web 3/24/2009

dynamics of CYP46A1 in solution upon interaction with different ligands, steroid substrates, and protein redox partner Adx.

Amide hydrogen−deuterium (H-D) exchange analyzed by mass spectrometry is a powerful tool for the analysis of protein conformation and dynamics in solution (*8*−*12*). Two ionization methods, electrospray ionization (ESI) and matrix-assisted laser desorption ionization (MALDI) are typically used in the H-D exchange experiments. The MALDI-based approach usually has a lower coverage of protein sequence and higher rate of back-exchange than the ESI-based approach but a higher speed of spectral acquisition, more straightforward peak assignment, and simpler data analysis. MALDI H-D exchange has been broadly used to study conformational changes in peptides (*13*−*15*), protein aggregation (*16*,*17*), epitope mapping of a monoclonal antibody (*18*), protein−membrane interaction (*19*), thermodynamics of protein−ligand complexes (*20*−*23*), and dynamics of various proteins in different states (*24*−*34*). The data obtained by MALDI H-D exchange are in good agreement with the data available from crystal structures (*27*−*34*). In the present work, we demonstrate that the MALDI H-D exchange is well suited to detect ligand-induced conformational changes in CYP46A1. We were able to identify and compare regions of the P450 affected by the binding of cholesterol sulfate, cholesterol, 24*S*-hydroxycholesterol, and Adx and through these studies enhance our understanding of how substrate binding affects the interaction between the P450 and the redox partner and how the redox partner affects binding of the substrate.

EXPERIMENTAL PROCEDURES

Materials. Deuterium oxide (99.96%) was purchased from Cambridge Isotope Laboratories (Andover, MA), immobilized pepsin from Pierce Chemicals (Rockford, IL), cholesterol and 24*S*-hydroxycholesterol from Avanti Polar Lipids (Alabaster, AL), and ZipTip C_{18} tips from Millipore (Bedford, MA). All other chemicals were from Sigma-Aldrich (St. Louis, MO). Prior to digestion, beads of immobilized pepsin were prewashed twice with 1 mL of cold 0.03% TFA (pH 2.5) and resuspended in cold 0.03% TFA.

Proteins. The truncated form, (Δ2−50), of recombinant human CYP46A1 was expressed as described (*35*). To obtain substrate-bound CYP46A1, enzyme purification was carried out in the presence of a selected steroid (*35*), namely, 50 μM cholesterol sulfate, 30 μM cholesterol, or 50 μM 24*S*-hydroxycholesterol. After the last purification step, CYP46A1 was diluted and concentrated several times to decrease the concentration of NaCl present in the buffer to 25 mM and adjust the ratio of steroid to CYP46A1 to 1:1. Recombinant bovine adrenodoxin was expressed and purified as described (*36*).

H-D Exchange. To initiate deuterium incorporation into substrate-free and steroid-bound CYP46A1, 5 μL of 40 μM protein (200 pmol) was mixed with 95 μL of the labeling buffer and 50 mM potassium phosphate (pD 7.2, in 95% D_2O). At certain time points, 10 μL of solution (20 pmol of CYP46A1) was removed and quenched with 10 μL of chilled 0.45% TFA. The final pH of the quenched sample was 2.5, and the sample was immediately frozen on dry ice/ethanol and stored at −80 °C until further analysis. Before the analysis, the quenched sample (20 μL) was thawed on ice for 5 min, mixed with 4 μL of prewashed immobilized pepsin slurry, and digested for 6 min on ice with occasional mixing. Beads of immobilized pepsin were then removed by centrifugation at 10,000*g* for 20 s, and the supernatant was applied to the ZipTip C_{18} tip. The tip was washed with 0.03%TFA, and peptides were eluted with 20% acetonitrile then 50% acetonitrile, each containing 0.03%TFA. Each fraction was mixed 1:1 (v/v) with a chilled matrix solution containing 6 mg/mL α-cyano-4-hydroxycinnamic acid, 40% acetonitrile, and 0.03% TFA. The mixture was quickly spotted onto a chilled stainless steel target plate. After 1 min, when peptides−matrix crystals precipitated, extra liquid was absorbed from the edge of each spot using tissues. The plate was immediately loaded into the mass spectrometer, and data were acquired without delay. All manipulations beginning from sample thawing to spotting the peptides onto the target plate were carried out at 4 °C in a cold room.

To probe the CYP46A1 dynamics upon Adx binding, 200 pmol of cholesterol-sulfate-bound or substrate-free CYP46A1 and 2 nmol (10-fold molar excess) of Adx were incubated in a total volume of 10 μL for 10 min at room temperature. To initiate deuterium incorporation, the reaction mixture was then diluted 20-fold into 50 mM potassium phosphate (pD 7.2, in 95% D_2O). Sample collection, quenching, pepsin digestion, ZipTip C_{18} separation, and spotting onto the target plate were performed exactly the same as described above.

MALDI-TOF MS. The MALDI-TOF mass spectra were acquired using a 4700 Proteomics Analyzer (Applied Biosystems, Framingham, MA). For initial assignment of peptic fragments, a peptic digest of CYP46A1 was prepared using the same digestion and handling conditions that were used for deuterium exchange experiments. The following identification of peptic fragments was performed on the basis of exact mass and MS/MS analysis. MS-mode acquisitions consisted of 2,400 laser shots averaged from 30 sample positions in each spot. In the MS/MS-mode acquisitions, 6,000 laser shots were averaged from 60 sample positions in each spot. The signal intensity threshold was set to a signal-to-noise ratio of 10. The precursor ion selection window was set at a resolution of 150, which is a typical setting for this instrument. Automated acquisition of MS and MS/MS data was controlled by 4000 Series Explorer software 3.0. MS spectra were internally calibrated in a two-point procedure using reference peptides with m/z $[M + H]^+$ values 976.5210 and 1891.0588. These peptides had been previously identified by MS/MS analysis. After calibration, MS spectra were manually analyzed on the basis of matching the observed masses with the theoretical masses of CYP46A1 peptides generated by FindPept software (http://us.expasy.org/tools/findpept.html) for pepsin digestion (pH > 2) with 4 missed cleavages. The observed m/z $[M + H]^+$ values deviated from the theoretical m/z $[M + H]^+$ values by no more than 10 ppm. Each identified peptide was also systematically interrogated by MS/MS analysis, and each

MS/MS spectrum was manually interpreted to validate the peptide.

Deuterium incorporation was determined by calculating the centroid of each isotopic peak cluster. The centroids were computed using the DEX software package (*37*); the centroid is a weighted average of the m/z values of the peaks in the isotopic envelope, with the weights equal to the corresponding peak areas. Deconvolution was performed using the natural isotopic distribution.

Back-exchange was estimated by measuring deuterium incorporation in a model peptide: KAQYARSVLLEKDAEPDILELATGYR (peptide B, NIST Reference Material 2397). This peptide was deuterated for 3 h and digested using the same handling conditions that were used for the CYP46A1 H-D exchange experiments. The ratio between deuterium incorporation and the total number of exchangeable backbone amide hydrogens for two peptic fragments of 1028.51 and 1034.59 Da was calculated and represents the back-exchange. The average of three experiments showed that the deuterium loss during the analysis was 48 ± 2% for both peptic fragments. Since all experiments were carried out under identical experimental conditions, the data obtained were not adjusted for the back-exchange (*10*).

Data Analysis. The full set of data used to determine if a peptide experienced a significant change in deuterium incorporation upon substrate or Adx binding is in the Supporting Information. Significance was not determined by a specific statistical test. Instead, we attempted to apply the same rules, described below, to each determination in an unbiased fashion.

Variation due to the ZipTip C_{18} separation and sample/matrix spotting sometimes caused a replicate experiment to give a low intensity or obscured mass spectrum for a particular peptide at one or more time points. The relative deuterium incorporation at these time points either could not be determined or had a distorted deuterium uptake curve. Uptake curves with few time points were discarded. Peptides with significant differences between the control and treatment groups were then identified as follows. First, among the three replicate experiments for each peptide, the two replicate experiments with the most similar deuterium uptake curves were selected. Next, the mean difference in deuterium incorporation between the control time points and the treatment time points were plotted for each peptide (Figures S1 and S2 in Supporting Information). Specifically, for a given peptide, the difference between each control/treatment pair in both replicate experiments was determined, and then the mean of these differences was calculated. These plots served as a guide for selecting the peptides that experienced a significant change in deuterium incorporation upon treatment. Generally, peptides with a mean difference greater than 0.5 were selected. However, to make a final decision for each peptide, the deuterium uptake curves for both replicate experiments were compared (Figures S3 to S17 in Supporting Information). Generally, both replicate experiments had to indicate a significant difference between the control and treatment to classify the peptide as experiencing a change in deuterium incorporation upon substrate or Adx binding. The exceptions were peptides 260−270 and 364−373 in 24*S*-hydroxycholesterol treatment and peptides 301−313 and 351−361 in Adx treatment. These exceptions are discussed in Supporting Information.

Analysis of the DEX output was performed using the R programming language (*38*), Microcal Origin 6.0 (OriginLab, Northhampton, MA), and PyMOL (DeLano Scientific LLC, South San Francisco, CA).

RESULTS

Peptide Mapping and Sequence Coverage of CYP46A1. To improve sequence coverage, the peptic peptides were first fractionated on ZipTip C_{18} tips by using a two-step elution with 20% acetonitrile followed by 50% acetonitrile. Subsequent accurate mass measurements of peptide ions and sequence information from the MS/MS fragmentation made it possible to assign monoisotopic masses to specific CYP46A1 peptides in each fraction. A total of 53 peptide fragments whose isotopic envelopes were well resolved after the H-D exchange were considered. These peptides cover most secondary structural elements in CYP46A1 and represent 83% of the protein sequence (Figure 1). The regions of CYP46A1 that were lost and not analyzed include residues 81−108 (the β1−2 sheet/B helix), 281−293 (H−I loop), and 406−425 (K″ helix) (Figure 1).

H-D Exchange of Cholesterol-Sulfate-Bound CYP46A1. The deuterium incorporation into substrate-bound CYP46A1 was compared to that of the substrate-free CYP46A1. Eleven peptides were found to have a change in deuterium uptake upon cholesterol sulfate binding (Figure 2). Six of these peptides (65−80, 109−116, 117−125, 225−239, 362−373, and 364−373) contain residues (F80, M108, Y109, R110, A111, L112, F121, N227, A367, W368, and F371) that interact with cholesterol sulfate in the crystal structure of cholesterol-sulfate-bound CYP46A1(*7*). The other five peptides (50−64, 129−143, 151−164, 351−361, and 445−455) are away from the active site. All 11 peptides that showed altered H-D exchange in solution represent the regions in CYP46A1 that were affected by cholesterol sulfate binding in the enzyme crystal structure (Figure 3). Also, the largest occurrences of deuteration in solution were observed for the most dynamic elements of the CYP46A1 crystal structure (peptides 50−64, 65−80, 109−116, and 225−239). These results suggested that the MALDI-based H-D exchange provides meaningful data and that the conformational differences between the cholesterol-sulfate-bound and substrate-free crystal structures of CYP46A1 (*7*) indeed reflect the substrate-induced conformational changes occurring in the protein in solution. These studies with cholesterol sulfate established the applicability of the H-D exchange methodology for elucidation of the molecular dynamics of CYP46A1 in solution and gave impetus to the investigation of cholesterol and 24*S*-hydroxycholesterol binding. Crystal structures of cholesterol- and 24*S*-hydroxycholesterol-bound CYP46A1 are not yet available.

H-D Exchange of Cholesterol- and 24S-Hydroxycholesterol-Bound CYP46A1. As in the case with cholesterol sulfate, deuterium incorporation was compared

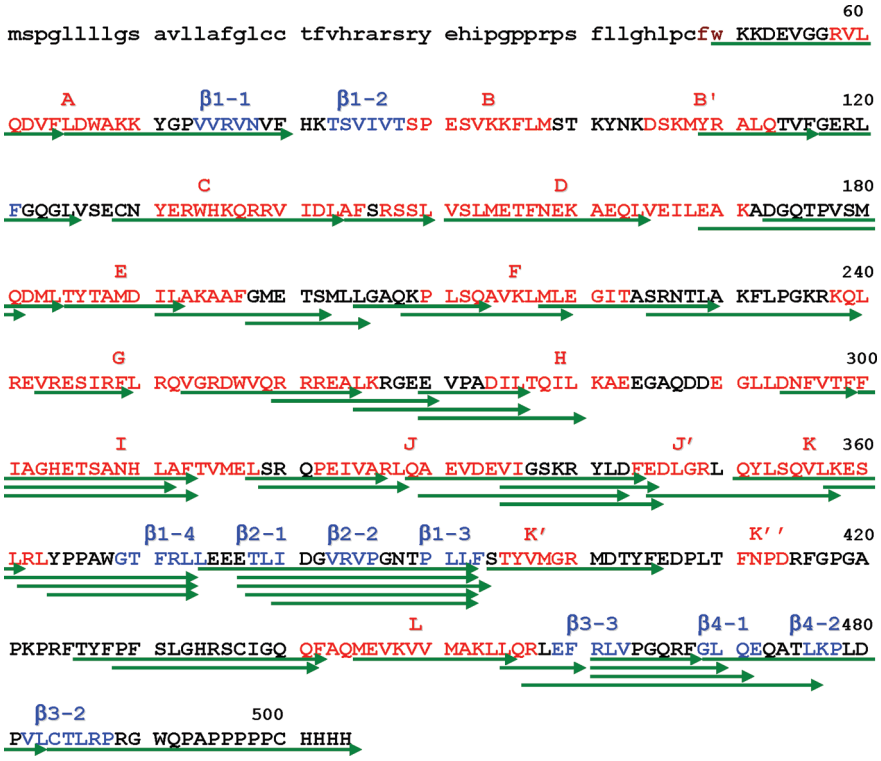

FIGURE 1: Sequence coverage of human CYP46A1 by peptic digestion. The peptides considered suitable for obtaining H-D exchange data are indicated by arrows and cover 83% of the (Δ2−50) CYP46A1 sequence. The secondary structural elements are shown above the sequence. Helixes and sheets are shown in red and blue, respectively.

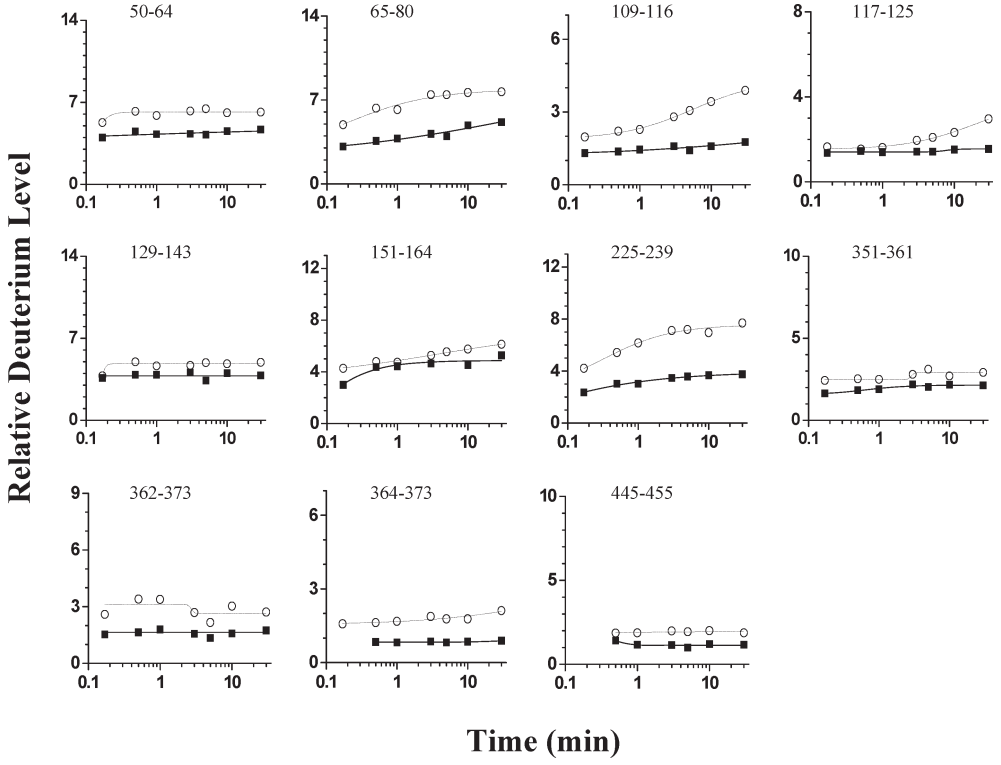

FIGURE 2: Peptides showing altered H-D exchange upon binding of cholesterol sulfate. The scale of the *y* axis shows the expected number of deuterated amide groups in each peptide. Adjustment for the back-exchange was not performed; therefore, the difference in deuterium incorporation between substrate-free (○) and cholesterol-sulfate-bound (■) CYP46A1 is a relative value.

to that of the substrate-free CYP46A1. Only four peptides (65−80, 109−116, 151−164, and 351−361) showed altered H-D exchange upon cholesterol binding (Figure 4). These peptides also exhibited changes in H-D exchange in cholesterol-sulfate-bound CYP46A1. Yet in cholesterol-bound CYP46A1, deuterium incorporation was smaller than that in the cholesterol-sulfate-bound enzyme.

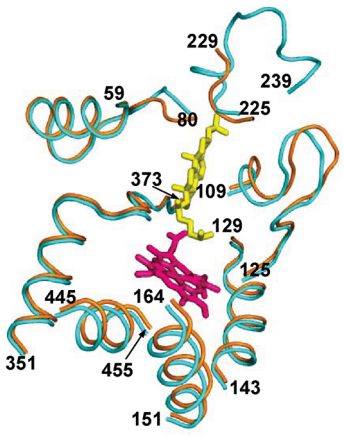

FIGURE 3: Regions in the CYP46A1 structure showing altered deuterium incorporation upon binding of cholesterol sulfate. Substrate-free CYP46A1 is in orange, cholesterol-sulfate-bound is in cyan, cholesterol sulfate is in yellow, and heme is in pink. The 230−239 region is disordered in substrate-free CYP46A1 and is therefore not shown.

Interaction with 24*S*-hydroxycholesterol elicited H-D exchange similar to that observed upon the binding of cholesterol sulfate. Eight peptides were identified (Figure 5). Seven of them are the same as those that showed altered deuterium uptake in cholesterol-sulfate-bound CYP46A1 (50−64, 65−80, 109−116, 117−125, 129−143, 151−164, and 364−373); however, one peptide (260−270) was different. This peptide may reflect a distinct feature of 24*S*-hydroxycholesterol binding to CYP46A1. Also, interaction with 24*S*-hydroxycholesterol did not affect deuteration of the 351−361 peptide, which showed changes in H-D exchange in cholesterol- and cholesterol-sulfate-bound CYP46A1.

Figures 2, 4, and 5 show mainly a decrease in H-D exchange suggesting a reduction in the flexibility of the protein backbone and/or shielding of the selected backbone protons by the substrate. Substrate-increased proton exchange of CYP46A1 was rare and observed only for the 364−373 peptide upon 24*S*-hydroxycholesterol-binding (Figure 5).

H-D Exchange of CYP46A1 Complex with Adx. Adx is a small 13 kDa soluble protein that transfers electrons to CYP46A1 in the *in vitro* reconstituted system. We used Adx as a model to gain insight into how substrate binding affects interaction of CYP46A1 with the redox partner. Unfortunately, we could not investigate the complex formation with CPR, the CYP46A1 natural redox partner. The sequence coverage of this complex was low in MALDI-based H-D exchange because both (Δ2−50) CYP46A1 and CPR are high molecular weight proteins (52 kDa and 78 kDa, respectively).

Substrate-free and cholesterol-sulfate-bound forms of CYP46A1 were used in the experiments with Adx. The results are summarized in Figure 6. Interaction with Adx affected the deuteration of five peptides in substrate-free CYP46A1 (144−150, 225−239, 265−276, 301−313, and 351−361). Three of these peptides (144−150, 265−276, and 301−313) also showed altered H-D exchange upon Adx binding in cholesterol-sulfate-bound CYP46A1. The 225−239 peptide that had the largest decrease in deuterium incorporation in the substrate-free CYP46A1−Adx complex was unaffected in cholesterol-sulfate-bound CYP46A1. As for the 351−361 peptide, unlike experiments with substrate-free CYP46A1, we could not find this peptide in cholesterol-sulfate-bound CYP46A1. On the basis of our mutagenesis studies, the 351−361 peptide represents a portion of the Adx-binding site in CYP46A1 (Pikuleva, I. A., personal communication).

In contrast to substrate binding that mainly led to a decrease in H-D exchange, Adx binding increased the H-D exchange in three of the five peptides identified in substrate-free CYP46A1 and all three peptides in cholesterol-sulfate-bound CYP46A1.

DISCUSSION

In the present work, we utilized H-D exchange mass spectrometry to study CYP46A1, an important enzyme that controls cholesterol elimination from the brain. We capitalized on the availability of substrate-free and substrate (cholesterol sulfate)-bound crystal structures of CYP46A1 (*7*) and comparative analysis of these structures indicating that the enzyme active site is conformationally flexible. We first compared deuteration of cholesterol-sulfate-bound and substrate-free CYP46A1 in solution and identified peptides showing different deuterium incorporation. These peptides were then mapped on the crystal structures of CYP46A1 and found to coincide with the regions of structural changes occurring upon interaction with cholesterol sulfate (Figure 3). Such good correspondence to the crystallographic data suggested that the MALDI H-D exchange methodology can indeed be used for studies of CYP46A1−ligand interactions and justified subsequent experiments with cholesterol, 24-hydroxycholesterol, and Adx. A summary of the peptides exhibiting a change in deuterium uptake upon binding of each of the tested ligands is shown in Table 1.

Cholesterol binds weaker to CYP46A1 than cholesterol sulfate, and *in vitro* has an apparent $K_d \approx 10$ times higher than that of cholesterol sulfate (*7*). The catalytic efficiency of cholesterol hydroxylation by CYP46A1 is also lower in the *in vitro* reconstituted system (*7*). Likely because of weaker binding, only four peptides in CYP46A1 were found to have altered deuteration upon interaction with cholesterol (shown in red in Figure 7). Two of these peptides form a part of the CYP46A1 active site. They are located at the entrance (the 65−80 peptide, which forms a part of the helix A) and in the middle of the substrate binding cavity (the 109−116 peptide, which forms a part of the B′ helix) (Figure 7). The other two peptides are outside the active site and seem to be associated with the binding of the CYP46A1 redox partner Adx. The 351−361 peptide (helix K) contains K358, whose mutation to alanine abolishes cholesterol hydroxylation when the redox partner is Adx but has no effect on cholesterol hydroxylation when the redox partner is CPR (Pikuleva, I. A., personal communication). The 351−361 peptide also defines a side of the proximal channel (presumably water channel) that is formed upon binding of cholesterol sulfate and filled with a network of hydrogen-bonded water molecules (*39*). Our H-D exchange data indicate that cholesterol binding alters the deuteration of this region as well. As for the 151−164 peptide, residues

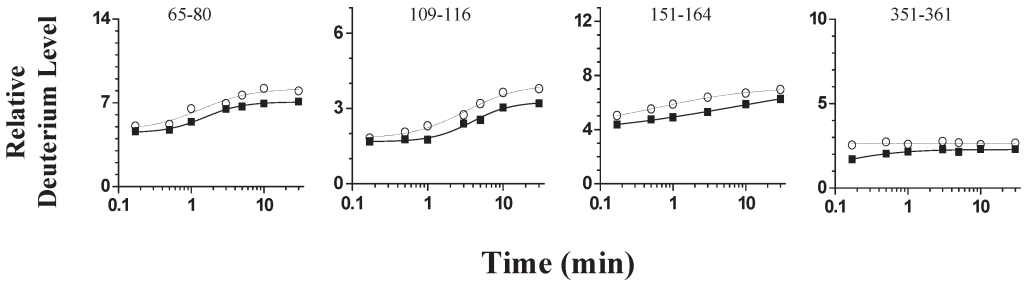

FIGURE 4: Peptides showing altered H-D exchange upon binding of cholesterol. The scale of the *y* axis shows the expected number of deuterated amide groups in each peptide. Adjustment for the back-exchange was not performed; therefore, the difference in deuterium incorporation between substrate-free (○) and cholesterol-bound (■) CYP46A1 is a relative value.

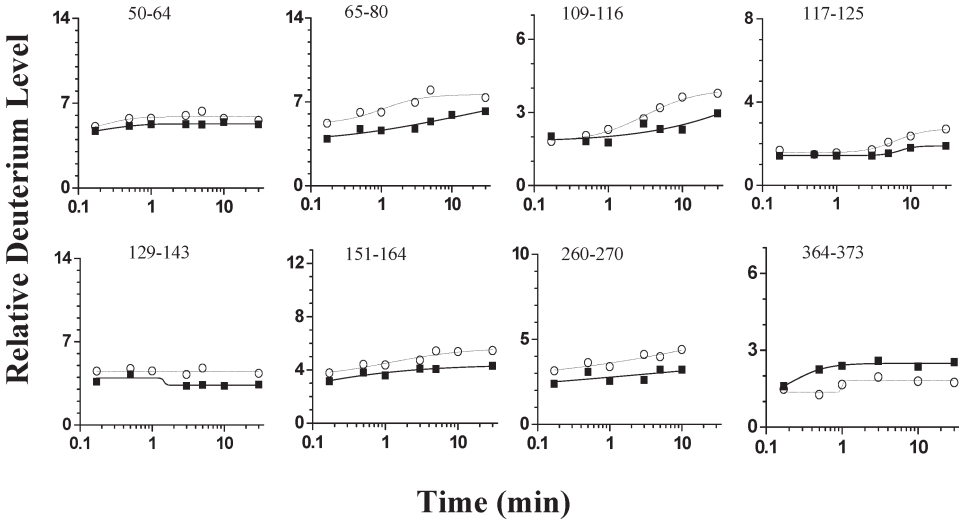

FIGURE 5: Peptides showing altered H-D exchange upon binding of 24*S*-hydroxycholesterol. The scale of the *y* axis shows the expected number of deuterated amide groups in each peptide. Adjustment for the back-exchange was not performed; therefore, the difference in deuterium incorporation between substrate-free (○) and 24*S*-hydroxycholesterol-bound (■) CYP46A1 is a relative value.

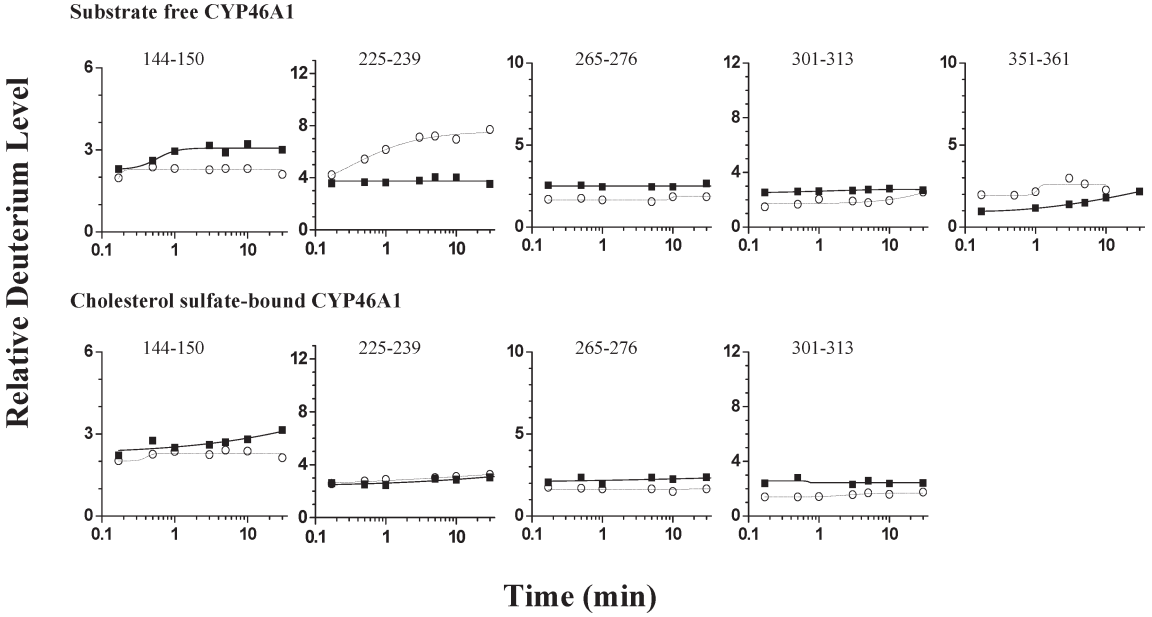

FIGURE 6: Peptides showing altered H-D exchange upon binding of Adx to substrate-free and cholesterol-sulfate-bound CYP46A1. The 225−239 peptide in cholesterol-sulfate-bound CYP46A1 is shown for comparison. The scale of the *y* axis shows the expected number of deuterated amide groups in each peptide. Adjustment for the back-exchange was not performed; therefore, the difference in deuterium incorporation in the absence (○) and presence (■) of Adx is a relative value.

within this peptide (that form a part of helix D) have not yet been mutated, but the neighboring R147 in the same helix was. As with the K358A mutation, the R147A substitution had no effect on cholesterol hydroxylation when the redox partner was CPR but reduced the rate of cholesterol hydroxylation ≈3-fold when the redox partner

Table 1: Summary of Peptides Showing Significant Change in Deuterium Uptake upon Ligand Binding[a]

peptide/ ligand	cholesterol sulfate	cholesterol	24*S*-hydroxy-cholesterol	Adx with substrate-free CYP46A1	Adx with cholesterol-sulfate-bound CYP46A1
50−64	X		X		
65−80	X	X	X		
109−116	X	X	X		
117−125	X		X		
129−143	X		X		
144−150				X	X
151−164	X	X	X		
225−239	X			X	
260−270			X		
265−276				X	X
301−313				X	X
351−361	X	X		X	
362−373	X				
364−373	X		X		
445−455	X				

[a] X indicates significance.

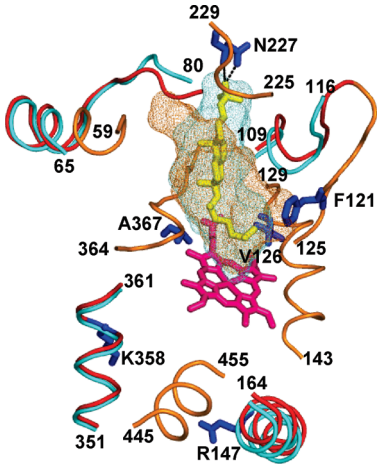

FIGURE 7: Regions in substrate-free CYP46A1 exhibiting altered deuterium incorporation upon binding of cholesterol (in red). Corresponding peptides in cholesterol-sulfate-bound are in cyan. Unaffected regions in substrate-free CYP46A1 are in orange. Cholesterol sulfate is in yellow, and heme is in pink. F121, V126, R147, N227, A367, and K358 are in blue. The shape of the active site in substrate-free CYP46A1 is shown in orange mesh and in cholesterol-sulfate-bound P450 in cyan mesh.

was Adx (Pikuleva, I. A., personal communication). R147, V151, M154, N158, E162, and E166 in the D helix form a network of hydrogen bonds via their backbone atoms. Consequently, cholesterol-induced changes in the 151−164 peptide may affect the position of the side chain of R147 and thus the interaction with Adx.

A number of peptides having altered deuterium incorporation upon cholesterol sulfate binding did not show changes in deuterium uptake upon cholesterol binding (Table 1). The lack of changes in deuteration of the 117−125 (B′-C loop) and 364−373 (β4−1 sheet) peptides that contain F121, V126, and A367, which restrain the side chain of cholesterol sulfate, suggests a different position of the steroid side chain in cholesterol-bound CYP46A1 (Figure 7). Also, the lack of changes in the 225−239 peptide (forms a part of the F-G loop) that contains

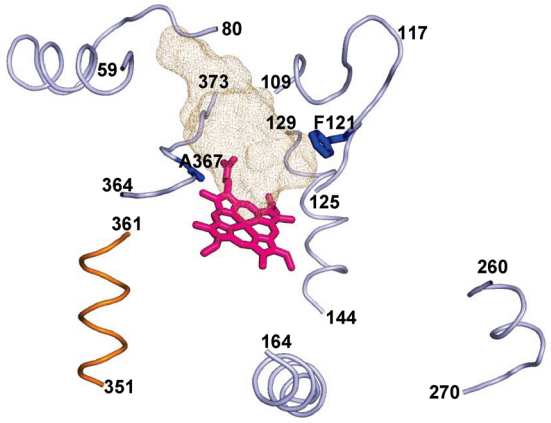

FIGURE 8: Regions in substrate-free CYP46A1 exhibiting altered deuterium incorporation upon binding of 24*S*-hydroxycholesterol (in light blue). The unaffected 351−361 peptide is in orange. Heme is in pink, A367 and F121 are in blue, and the shape of the active site in substrate-free CYP46A1 is in olive mesh.

N227 hydrogen bonded to the sulfate anion in cholesterol sulfate indicates that the cholesterol 3β-hydroxyl does not interact with the residues in the F-G loop. Finally, cholesterol binding did not affect the deuteration of the 445−455 peptide, one of the two peptides that form the proximal channel in cholesterol-sulfate-bound CYP6A1 (*39*), but reduced the deuterium uptake of the other 351−361 peptide. It is possible that the hydration of the CYP46A1 active site in cholesterol-bound and cholesterol-sulfate-bound enzymes is different. Cholesterol seems to induce smaller conformational changes in CYP46A1 than cholesterol sulfate, suggesting that the shape of the active site in cholesterol-bound CYP46A1 is more similar to that of the substrate-free enzyme than that of the cholesterol-sulfate-bound form (Figure 7). The major differences from the substrate-free CYP46A1 appear to be at the entrance and in the middle of the substrate access channel where the cholesterol 3β-hydroxyl and steroid nucleus interact with the residue(s)/backbone of CYP46A1. The similarity with cholesterol-sulfate-bound CYP46A1 includes conformational changes in or close to the sites of the redox partner binding and around the water channel. Identification of these conformational changes is an important finding for the P450 field because it provides first structural insight into how substrate binding affects interaction with the redox partner and hydration of the P450 active site.

24*S*-Hydroxycholesterol binds tighter to CYP46A1 than cholesterol and is a better substrate for CYP46A1 than cholesterol (*6*,*7*). The tighter binding of 24*S*-hydroxycholesterol is probably due to the additional interaction(s) provided by the 24*S*-hydroxyl group. Probably due to these additional interaction(s), the two peptides, 117−125 and 364−373, that contain F121 and A367 that define the position of the steroid side chain (Figure 8) and are unaffected by cholesterol binding, had altered H-D exchange upon 24*S*-hydroxycholesterol binding. The 117−125 peptide showed a decreased deuterium uptake, whereas the deuteration of the 364−373 peptide was increased. These results suggest that the side chain of 24*S*-hydroxycholesterol will be closer to the 117−125 peptide but farther from the 364−373 peptide than the side chain of cholesterol. Unlike cholesterol sulfate and cholesterol, 24*S*-hydroxycholesterol did not elicit changes

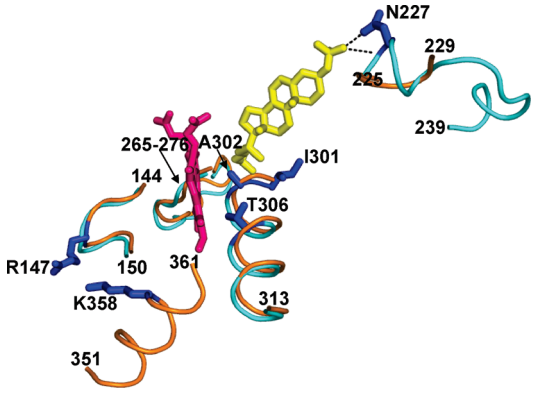

FIGURE 9: Regions in CYP46A1 affected by the binding of Adx. Peptides in substrate-free CYP46A1 are shown in orange and in cholesterol-sulfate-bound P450 in cyan. Cholesterol sulfate is in yellow, heme is in pink, R147, N227, I301, A302, T306, and K358 are in blue. The 230−239 region is disordered in substrate-free CYP46A1 and is therefore not shown.

in the deuteration of the 351−361 peptide but reduced deuterium uptake of the 260−270 peptide. The former is putatively involved in the interaction with Adx and also forms the entrance to the proximal channel; the function of the latter (which forms the C-terminal part of helix G) is unknown. These distinct features of 24*S*-hydroxycholesterol binding, lack of changes in the H-D exchange of the 351−361 peptide and reduced deuteration of the 260−270, may explain our previous observation pertinent to substrate dependence of the CYP46A1 redox partner interactions. We found that the catalytic efficiency of cholesterol hydroxylation is ≈3-fold higher with Adx as a redox partner than with CPR, whereas for 24*S*-hydroxycholesterol hydroxylation, CPR is a much better redox partner than Adx (Pikuleva, I. A., personal communication). The H-D exchange behavior of 24*S*-hydroxycholesterol-bound CYP46A1 suggests that 24*S*-hydroxycholesterol does not prepare CYP46A1 for efficient binding of Adx or maybe even deteriorates the interaction with this redox partner.

We also tested how binding of one of the CYP46A1 substrates, cholesterol sulfate, affects interaction with Adx. Two peptides were affected, 225−239 and 351−361. The 225−239 peptide forms a part of the F-G loop, which is disordered in substrate-free CYP46A1 but becomes more stabilized in cholesterol-sulfate-bound CYP46A1 because N227 forms two hydrogen bonds with the sulfate anion (Figure 9). Binding of Adx made the F-G loop less dynamic in substrate-free CYP46A1 but had no effect on this region in the cholesterol-sulfate-bound enzyme, which is already stabilized by the interaction with the substrate. Also, interaction with Adx reduced deuteration of the 351−361 peptide in substrate-free CYP46A1, but we could not recover this peptide in all three experiments with the cholesterol-sulfate-bound enzyme. Reduced deuterium uptake of the 351−361 peptide in substrate-free P450 is consistent with our mutagenesis studies suggesting that K358 in this peptide interacts with Adx. The lack of this peptide in the experiments with cholesterol-sulfate-bound CYP46A1 is more difficult to explain. Probably, simultaneous binding of cholesterol sulfate and Adx affected the CYP46A1 cleavage in this region, and the 351−361 peptide was not generated. Substrate-free and substrate-bound forms of CYP46A1 also showed similarities in H-D exchange in the presence of Adx. Reduced deuteration of the 144−150 peptide (the N-terminal part of the F helix) is consistent with our mutagenesis data suggesting the involvement of R147 in the binding of Adx. Altered deuterium uptake of the 265−276 (the G-H loop) and 301−313 (a part of the I helix) peptides is a novel finding. The 265−276 peptide is spatially close to the 144−150 peptide (Figure 9). It is possible that interaction of Adx with R147 also affects the neighboring 265−276 peptide. The 301−313 peptide constitutes a part of the active site with I301, A302, and T306 defining the position of the side chain of cholesterol sulfate over the heme iron, the site of catalysis (*7*). In the crystal structure of CYP46A1, C24 and C25 of cholesterol sulfate, the primary and secondary sites, respectively, of hydroxylation, are positioned at a 5.7 Å distance from the heme iron, which is ∼1−1.5 Å greater than expected for hydroxylation of the oxyferryl intermediate during turnover (*40*). The reduced H-D exchange of the 301−313 peptide suggests that binding of the redox partner makes the substrate side chain or the whole steroid molecule move closer to the I helix and consequently the heme iron.

In summary, by using H-D exchange and mass spectrometry, we identified unique and common regions in CYP46A1 undergoing conformational changes upon binding of steroid substrates and the protein redox partner Adx. We gained structural insight into how substrate binding may affect the hydration of the P450 active site and why redox partner preferences of CYP46A1 depend on the steroid used. Results of the H-D exchange mass spectrometry become particularly informative when combined with the data obtained by other methods.

ACKNOWLEDGMENT

Certain commercial materials, instruments, and equipment are identified in this manuscript in order to specify the experimental procedure as completely as possible. In no case does such identification imply a recommendation or endorsement by the National Institute of Standards and Technology (NIST) nor does it imply that the materials, instruments, or equipment identified is necessarily the best available for the purpose.

SUPPORTING INFORMATION AVAILABLE

The mean difference in deuterium incorporation between the control and treatment time points for the substrate and Adx binding experiments and selected duplicates of the deuterium uptake curves for the peptides presented in Table 1. This material is available free of charge via the Internet at http://pubs.acs.org.

REFERENCES

1. Pikuleva, I. A. (2006) Cytochrome P450s and cholesterol homeostasis. *Pharmacol. Ther. 112*, 761–773.
2. Pikuleva, I. A. (2006) Cholesterol-metabolizing cytochromes P450. *Drug Metab. Dispos. 34*, 513–520.
3. Lund, E. G., Guileyardo, J. M., and Russell, D. W. (1999) cDNA cloning of cholesterol 24-hydroxylase, a mediator of cholesterol homeostasis in the brain. *Proc. Natl. Acad. Sci. U.S.A. 96*, 7238–7243.
4. Bjorkhem, I., Andersson, U., Ellis, E., Alvelius, G., Ellegard, L., Diczfalusy, U., Sjovall, J., and Einarsson, C. (2001) From brain to bile. Evidence that conjugation and ω-hydroxylation are important

for elimination of 24*S*-hydroxycholesterol (cerebrosterol) in humans. *J. Biol. Chem. 276*, 37004–37010.
5. Janowski, B. A., Grogan, M. J., Jones, S. A., Wisely, G. B., Kliewer, S. A., Corey, E. J., and Mangelsdorf, D. J. (1999) Structural requirements of ligands for the oxysterols liver X receptors LXRα and LXR*β*. *Proc. Natl. Acad. Sci. U.S.A. 96*, 266–271.
6. Mast, N., Norcross, R., Andersson, U., Shou, M., Nakayama, K., Bjorkhem, I., and Pikuleva, I. A. (2003) Broad substrate specificity of human cytochrome P450 46A1 which initiates cholesterol degradation in the brain. *Biochemistry 42*, 14284–14292.
7. Mast, N., White, M. A., Bjorkhem, I., Johnson, E. F., Stout, C. D., and Pikuleva, I. A. (2008) Crystal structure of substrate-bound and substrate-free cytochrome P450 46A1, the principal cholesterol hydroxylase in the brain. *Proc. Natl. Acad. Sci. U.S.A. 105*, 9546–9551.
8. Busenlehner, L. S., and Armstrong, R. N. (2005) Insights into enzyme structure and dynamics elucidated by amide H/D exchange mass spectrometry. *Arch. Biochem. Biophys. 433*, 34–46.
9. Engen, J. R. (2003) Analysis of protein complexes with hydrogen exchange and mass spectrometry. *Analyst 128*, 623–628.
10. Wales, T. E., and Engen, J. R. (2006) Hydrogen exchange mass spectrometry for the analysis of protein dynamics. *Mass Spectrom. Rev. 25*, 158–170.
11. Hoofnagle, A. N., Resing, K. A., and Ahn, N. G. (2003) Protein analysis by hydrogen exchange mass spectrometry. *Annu. Rev. Biophys. Biomol. Struct. 32*, 1–25.
12. Tsutsui, Y., and Wintrode, P. L. (2007) Hydrogen/deuterium exchange-mass spectrometry: a powerful tool for probing protein structure, dynamics and interactions. *Curr. Med. Chem 14*, 2344–2358.
13. Figueroa, I. D., and Russell, D. H. (1999) Matrix-assisted laser desorption ionization hydrogen/deuterium exchange studies to probe peptide conformational changes. *J. Am. Soc. Mass Spectrom. 10*, 719–731.
14. Kipping, M., and Schierhorn, A. (2003) Improving hydrogen/deuterium exchange mass spectrometry by reduction of the back-exchange effect. *J. Mass Spectrom. 38*, 271–276.
15. Oliva, A., Llabres, M., and Farina, J. B. (2007) Application of matrix-assisted laser desorption/ionization time-of-flight mass spectrometry and hydrogen exchange combined with enzymatic digestion for the structural characterization of antimalaric Apf66 peptide. *Talanta 72*, 1192–1198.
16. Nazabal, A., Reis, S. D., Bonneu, M., Saupe, S. J., and Schmitter, J.-M. (2003) Conformational transition occurring upon amyloid aggregation of the HET-s prion protein of *Podospora anserine* analyzed by hydrogen/deuterium exchange and mass spectrometry. *Biochemistry 42*, 8852–8861.
17. Nazabal, A., and Schmitter, J.-M. (2006) Hydrogen-deuterium exchange analyzed by matrix-assisted laser desorption-ionization mass spectrometry and the HET-s prion model. *Methods Enzymol. 413*, 167–181.
18. Baerga-Ortiz, A., Hughes, C. A., Mandell, J. G., and Komives, E. A. (2002) Epitope mapping of a monoclonal antibody against human thrombin by H/D-exchange mass spectrometry reveals selection of a diverse sequence in a highly conserved protein. *Protein Sci. 11*, 1300–1308.
19. Man, P., Montagner, C., Vernier, G., Dublet, B., Chenal, A., Forest, E., and Forge, V. (2007) Defining the interacting regions between apomyoglobin and lipid membrane by hydrogen/deuterium exchange coupled to mass spectrometry. *J. Mol. Biol. 368*, 464–472.
20. Powell, K. D., and Fitzgerald, M. C. (2004) High-throughput screening assay for the tunable selection of protein ligands. *J. Comb. Chem. 6*, 262–269.
21. Ma, L., and Fitzgerald, M. C. (2003) A new H/D exchange- and mass spectrometry-based method for thermodynamic analysis of protein-DNA interactions. *Chem. Biol. 10*, 1205–1213.
22. Tang, L., Roulhac, P. L., and Fitzgerald, M. C. (2007) H/D exchange and mass spectrometry-based method for biophysical analysis of mutidomain proteins at the domain level. *Anal. Chem. 79*, 8728–8739.
23. Roulhac, P. L., Weaver, K. D., Adhikari, P., Anderson, D. S., DeArmond, P. D., Mietzner, T. A., Crumbliss, A. L., and Fitzgerald, M. C. (2008) *Ex vivo* analysis of synergistic anion binding to FbpA in Gram-negative bacteria. *Biochemistry 47*, 4298–4305.
24. Johnson, R. S., and Walsh, K. A. (1994) Mass spectrometric measurement of protein amide hydrogen exchange rates of apo- and holo-myoglobin. *Protein Sci. 3*, 2411–2418.
25. Mandell, J. G., Falick, A. M., and Komives, E. A. (1998) Measurement of amide hydrogen exchange by MALDI-TOF mass spectrometry. *Anal. Chem. 70*, 3987–3995.
26. Mandell, J. G., Baerga-Ortiz, A, Akashi, S., Takio, K., and Komives, E. A. (2001) Solvent accessibility of the thrombin-thrombomodulin interface. *J. Mol. Biol. 306*, 575–589.
27. Turner, B. T.Jr., and Maurer, M. C. (2002) Evaluating the roles of thrombin and calcium in the activation of coagulation factor XIII using H/D exchange and MALDI-TOF MS. *Biochemistry 41*, 7947–7954.
28. Koeppe, J. R., and Komives, E. A. (2006) Amide H/^{2}H exchange reveals a mechanism of thrombin activation. *Biochemistry 45*, 7724–7732.
29. Anand, G. S., Hotchko, M., Brown, S. H. J., Ten Eyck, L. F., Komives, E. A., and Taylor, S. S. (2007) R-subunit isoform specificity in protein kinase A: distinct features of protein interfaces in PKA types I and II by amide H/^{2}H exchange mass spectrometry. *J. Mol. Biol. 374*, 487–499.
30. Sabo, T. M., Brasher, P. B., and Maurer, M. C. (2007) Perturbations in factor XIII resulting from activation and inhibition examined by solution based methods and detected by MALDI-TOF MS. *Biochemistry 46*, 10089–10101.
31. Gu, Z., Zitzewitz, J. A., and Matthews, C. R. (2007) Mapping the structure of folding cores in TIM barrel proteins by hydrogen exchange mass spectrometry: the roles of motif and sequence for the indole-3-glycerol phosphate synthase from *Sulfolobus solfataricus*. *, J. Mol. Biol. 368*, 582–594.
32. Laine, O., Streaker, E. D., Nabavi, M., Fenselau, C. C., and Beckett, D. (2008) Allosteric signaling in the biotin repressor occurs via local folding coupled to global dampening of protein dynamics. *J. Mol. Biol. 381*, 89–101.
33. Alverdi, V., Mazon, H., Versluis, C., Hemrika, W., Esposito, G., van den Heuvel, R., Scholten, A., and Heck, A. J. R. (2008) cGMP-binding prepares PKG for substrate binding by disclosing the C-terminal domain. *J. Mol. Biol. 375*, 1380–1393.
34. Schuster, M. C., Ricklin, D., Papp, K., Molnar, K. S., Coales, S. J., Hamuro, Y., Sfyroera, G., Chen, H., Winters, M. S., and Lambris, J. D. (2008) Dynamic structural changes during complement C3 activation analyzed by hydrogen/deuterium exchange mass spectrometry. *Mol. Immunol. 45*, 3142–3151.
35. White, M. A., Mast, N., Bjorkhem, I., Johnson, E. F., Stout, C. D., and Pikuleva, I. A. (2008) Use of complementary cation and anion heavy-atom salt derivatives to solve the structure of cytochrome P450 46A1. *Acta Crystallogr., Sect. D 64*, 487–495.
36. Pikuleva, I. A., Tesh, K., Waterman, M. R., and Kim, Y. (2000) The tertiary structure of full-length bovine adrenodoxin suggests functional dimers. *Arch. Biochem. Biophys. 373*, 44–55.
37. Hotchko, M., Anand, G. S., Komives, E. A., and Ten Eyck, L. F. (2006) Automated extraction of backbone deuteration levels from amide H/2H mass spectrometry experiments. *Protein Sci. 15*, 583–601.
38. R Development Core Team ((2008)) R: a language and environment for statistical computing, R Foundation for Statistical Computing, Vienna, Austria, http://www.R-project.org..
39. Pikuleva, I. A. (2008) Cholesterol-metabolizing cytochromes P450: implications for cholesterol lowering. *Expert Opin. Drug Metab. Toxicol. 4*, 1403–1414.
40. Poulos, T. L., and Johnson, E. F. ((2005)) In *Structures of Cytochrome P450 Enzymes* (Ortiz de Montellano, P. R., Ed.) 3rd ed., pp 87−114, Kluwer, New York.